

BR 433/222

ISSN 0029-3888



**CBPF** - CENTRO BRASILEIRO DE PESQUISAS FÍSICAS

---

---

## Notas de Física

CBPF-NF-007/92 ✓

FIRETUBE MODEL AND HADRON-HADRON COLLISIONS

by

R.A.M.S. NAZARETH, T. KODAMA and D.A. PORTES JR.

RIO DE JANEIRO

1992

**NOTAS DE FÍSICA é uma pré-publicação de trabalho original em Física**

**NOTAS DE FÍSICA is a preprint of original works unpublished in Physics**

**Pedidos de cópias desta publicação devem ser enviados aos autores ou a:**

**Requests for copies of these reports should be addressed to:**

**Centro Brasileiro de Pesquisas Físicas  
Área de Publicações  
Rua Dr. Xavier Sigaud, 150 - 4º andar  
22.290 - Rio de Janeiro, RJ  
BRASIL**

ISSN 0029-3865

CBPF-NF-007/92

FIRETUBE MODEL AND HADRON-HADRON COLLISIONS

by

R.A.M. S. NAZARETH<sup>\*</sup>, T. KODAMA<sup>1</sup> and D.A. PORTES JR.<sup>1</sup>

<sup>1</sup>Centro Brasileiro de Pesquisas Físicas - CBPF/CNPq  
Rua Dr. Xavier Sigaud, 150  
22290 - Rio de Janeiro, RJ - Brasil

<sup>\*</sup>Universidade Federal do Rio de Janeiro  
Instituto de Física  
Cidade Universitária - Ilha do Fundão  
21910 - Rio de Janeiro, RJ - Brasil

### Abstract

A new version of the firetube model is developed to describe hadron-hadron collisions at ultrarelativistic energies. Several improvements are introduced in order to include the longitudinal expansion of intermediate fireballs, which remedies the overestimates of the transverse momenta in the previous version. It is found that, within a wide range of incident energies, the model describes well the experimental data for the single particle rapidity distribution, two-body correlations in the pseudo-rapidity, transverse momentum spectra of pions and kaons, the leading particle spectra and the  $K/\pi$  ratio.

**Key-words:** Relativistic hadron-hadron collisions; Firetube model; Fireball decay.

## I. INTRODUCTION

A couple of years ago, we proposed a simple phenomenological model for the proton-proton(antiproton) collision process<sup>1-3</sup> based on a mechanism in which a chromodynamical firetube fragments into intermediate fireballs which subsequently decay isotropically into the observed hadrons. The model, in spite of its simplicity, was found to reproduce the experimental rapidity and pseudorapidity distributions of pions within a wide energy interval, extending from  $\sqrt{s} \sim 20\text{GeV}$  to  $\sqrt{s} \sim 1\text{TeV}$ . However, there exist some shortcomings of the model because of the oversimplified picture. For example, the fireball decay was assumed to be isotropic there, and this leads to an overestimate of the transverse momenta of the final pions.

Thus, we consider it worthwhile to improve the oversimplified picture of the original version, as well as to extend the model to calculate other quantities than pion rapidity distributions, such as kaon distributions and leading particle spectra. We also intend to reproduce the pion and kaon spectra in any hadron-hadron collisions other than  $p - p(\bar{p})$  reactions keeping the simple geometric extension of the model.

In § II, we describe the firetube model with several improvements. We first analyze the mass and rapidity distributions of fireballs and discuss them with respect to the rapidity correlations of pions. In our model, the leading particle spectra is directly related to those of the fireballs originated from the end-points of the firetube. From this picture, we can calculate the leading particle spectra and the inelasticity coefficient.

We also discuss there the decay mode of the fireballs into hadrons. The main improvement for the treatment of the fireball decay processes is the introduction of the effect of the longitudinal expansion of the fireballs on the final hadron spectra. This remedies the large transverse momentum caused by the simple isotropic decay hypothesis used in the original version<sup>3</sup>. Furthermore, the kaon degree of freedom is introduced in the decay mode. For this purpose, the  $K/\pi$  ratio is determined as a function of the fireball mass.

In § III, we determine the values of the adjustable parameters introduced in the model. Data analyzed here are (pseudo-)rapidity distributions of charged (or negatively charged) particles,  $p_t$  distributions of pions and kaons, the energy dependence of the average  $p_t$ , and  $K/\pi$  ratio. The results are discussed and compared with experimental data when available.

Some concluding remarks and comments are given in § IV.

## II. FIRETUBE MODEL OF HADRON-HADRON COLLISIONS

The phenomenological model developed in refs.<sup>1-3</sup> describes proton-proton collisions as a three-stage process. In the first part of the collision the protons become colored objects due to exchange of their sea quarks, generating a chromodynamical flux tube (firtube) between them. This firtube can be represented by a classical string with an effective string constant. In the next stage this tube fragments into a set of intermediate objects (fireballs), which subsequently decay into the observable hadrons. This model is similar to the one developed by the Lund group<sup>4</sup>, except that in the latter, hadrons are produced directly from the fragmentation of a string, without an intermediate fireball stage<sup>5</sup>. In what follows we present the main ingredients of the model in each stage.

### FIRETUBE FORMATION

One of the basic characters of the model is that the effective string constant  $\kappa$  of the firtube is taken as a function of the impact parameter and the incident energy. The tension coefficient is given by,

$$k_{eff} = \epsilon_0 A(b, \sqrt{s}), \quad (1)$$

where  $\epsilon_0$  is the volumetric energy density of the flux tube with transverse area  $A(b, \sqrt{s})$ . The transverse area of the effective string is proportional to the total hadron-hadron cross section times an universal function of the impact parameter  $b$ ,<sup>3</sup>

$$A(b, \sqrt{s}) = \sigma_{tot}(\sqrt{s}) f(b). \quad (2)$$

where

$$\frac{d^2 f(b)}{db^2} \equiv \frac{1}{\sigma} \frac{d^2 \sigma}{db^2}, \quad (3)$$

$A(b, \sqrt{s})$  is considered as the effective overlapping area between protons at impact parameter  $b$ . In Ref.3,  $A(b, \sqrt{s})$  was taken just as the geometric overlapping area of two flat disks. However, from the parton point of view, the effective energy density of the string should be proportional to the numbers of partons contributing to the inelastic process. In this aspect, the universal function is rather well approximated by a Gaussian one<sup>6</sup> than that of the simple geometric overlap of two disks. Thus we take

$$\frac{d^2 f(b)}{db^2} = \frac{\lambda}{\pi} e^{-\lambda b^2/b_{max}^2}, \quad (4)$$

where  $b_{max}$  is related to the total inelastic cross section as

$$\pi b_{max}^2 = \sigma_{inel}(\sqrt{s}), \quad (5)$$

and  $\lambda$  is determined by the condition<sup>6</sup>

$$\langle b^2 \rangle = 0.47 \left( \frac{b_{max}}{2} \right)^2$$

i.e.  $\lambda = 8.5$ .

Then, the motion of the two colored (excited) hadrons is described by the classical Hamiltonian

$$H(b) = (p_1^2 + m_{h_1}^2)^{1/2} + (p_2^2 + m_{h_2}^2)^{1/2} + k_{eff} |x_1 - x_2|, \quad (6)$$

where  $x_i$  and  $p_i$  are the coordinates and momenta of the particles at each end of the effective string and  $m_{h_1}$  and  $m_{h_2}$  are the mass thresholds of the excited hadrons (see later). The time evolution of the system is obtained by solving the equations of motion derived from the Hamiltonian, Eq.(6). The trajectories of the end-point particles are two intertwined hyperbolas.

## FIRETUBE FRAGMENTATION INTO FIREBALLS

Another basic ingredient of the model is the stochastic break up of the firetube at any space-time just like in the Lund string model<sup>4</sup>. We denote as  $\omega$ , the probability density  $d^2P/(dx dt)$  of the firetube break up.

The firetube breaking is related, in some way, to the spontaneous quark-antiquark pair production inside the firetube, but definitely it is not a perturbative process. It might be possible to relate  $\omega$  to the energy density of the firetube from some QCD inspired models. However we just take here the simplest choice, i.e,  $\omega$  constant and consider it just a simple phenomenological parameter to fit the data.

The firetube breaking process splits the original firetube into two sub-firetubes; their energy and momentum being determined by the precise point where the break takes place. This process may continue to occur in the sub-firetubes. When a sub-firetube does not break up within the first period of its  $y_0$ - $y_0$  cycle, it collapses into a point due to the string tension. At this point, we assume that all the kinetic energy of the string in its CM system is converted into internal energy of a highly excited object (fireball).

For a given  $\omega$  and the initial CM energy of the firetube, we thus can calculate analytically the mass and rapidity distributions of the fireballs<sup>3</sup>. However, the assumption of constancy

of  $\omega$  anywhere in space is obviously not appropriate near the end points of the firetube, since the boundary effects will certainly reduce the probability of breaking in order to inhibit the production of too small short sub-firetubes. In other words, we assume that the firetube breaking occurs only when the invariant mass of the resultant sub-firetube is greater than or equal to some threshold value  $m_{tA}$ . We consider  $m_{tA}$  as a parameter of the model.

In Ref.3 details of the firetube break up process are discussed so that we will not repeat them here. We just show in Figs.1-a,b, the calculated mass and rapidity distributions of the fireballs generated by the process of firetube break up. Note that the form of the mass distribution does not change appreciably with respect to the incident energy, although the higher the incident energy is, the more the heavy fireballs can appear. Consequently, the average size of fireballs increases slowly with the incident energy.

### CORRELATIONS IN RAPIDITY OF HADRONS

The forms of the mass and rapidity distributions are intimately related to the correlation of produced particles. The smallness of average fireball mass should generate a strong correlation in the rapidity spectrum of produced pions. In fact, phenomenological analyses of rapidity correlation pattern of produced particles in very high energy  $pp$  and  $p\bar{p}$  collisions suggest the existence of some mechanism of clustering in hadronization process<sup>7</sup>. Although a part of such clusters can be interpreted as hadron resonances, there seem to remain some of correlation pattern that can not be interpreted by hadron resonances. Since the observed hadrons are originated from these fireballs, we expect that the analysis of the two-particle correlation will provide a critical check to the mass and rapidity spectra of fireballs predicted by the model.

The two-particle correlation in pseudo-rapidity space is defined as

$$C(\eta_1, \eta_2) = \frac{1}{\sigma} \frac{d^2\sigma}{d\eta_1 d\eta_2} - \frac{1}{\sigma} \frac{d\sigma}{d\eta_1} \frac{1}{\sigma} \frac{d\sigma}{d\eta_2}; \quad (7)$$

It is further decomposed into two parts: the so-called short range and the long range correlations as<sup>7</sup>

$$C_S = \sum_n \frac{\sigma_n}{\sigma} \left\{ \frac{1}{\sigma_n} \frac{d^2\sigma_n}{d\eta_1 d\eta_2} - \frac{1}{\sigma_n} \frac{d\sigma_n}{d\eta_1} \frac{1}{\sigma_n} \frac{d\sigma_n}{d\eta_2} \right\}, \quad (8)$$

$$C_L = \sum_n \frac{\sigma_n}{\sigma} \left\{ \frac{1}{\sigma} \frac{d\sigma}{d\eta_1} - \frac{1}{\sigma_n} \frac{d\sigma_n}{d\eta_1} \right\} \left\{ \frac{1}{\sigma} \frac{d\sigma}{d\eta_2} - \frac{1}{\sigma_n} \frac{d\sigma_n}{d\eta_2} \right\}$$

where the subscript  $n$  indicates the quantity of given multiplicity  $n$ . It has been argued<sup>7</sup> that

the observed short range correlation pattern (see Fig.2) suggest the existence of clusters at the time of hadronization. Since the short range correlation is sensible to the size of the clusters, this will provide a good check of the mass distribution of the fireballs of our model. In order to see this effect, we calculated here the rapidity correlation of pions based on the fireball spectrum of the present model. The whole process of  $p-p$  and  $p-\bar{p}$  collisions are simulated by the Monte-Carlo method. The momenta of the final hadrons are generated according to the isotropic fireball decay<sup>3</sup>. The multiplicity distribution of hadrons of a fireball is taken to be a Poisson type with average multiplicity  $\langle n \rangle = 2.1\sqrt{M}$  where  $M$  is the fireball mass. In Fig.2, we compare the results to the experimental data for  $\sqrt{s}$  between 63 and 900 GeV. The solid lines are the results of the model, and the filled circles are the experimental values<sup>8</sup>. We see that the short range correlations are surprisingly well reproduced by the model for all energies. It is worthwhile to mention that in these calculations, no new adjustable parameters are introduced. We thus conclude that the present picture of the formation of intermediate fireballs with the predicted mass distribution of the firetube model is consistent to the short range rapidity correlation data.

On the other hand, the long range correlation is intimately related to the multiplicity fluctuations<sup>7</sup>. In the present calculation it is found that, due to the simple assumption of the Poisson distribution, the fluctuation in multiplicity of pions is smaller than the experimental one. This leads to an overall underestimate of the normalization factor in the long range correlation spectra<sup>9</sup>.

We also checked the influence of anisotropic decay of fireballs into pions on the correlation data<sup>9</sup>. We found that a longitudinally deformed decay mode improves the long range correlation data. This also improves the overestimate of average transverse momenta of produced pions as already pointed out in Ref.1. Therefore, it seems crucial to include the effect of longitudinal expansion of fireballs before they hadronize into hadrons. This will be discussed later in detail.

## LEADING PARTICLE SPECTRA

In our model, the incident hadrons are always attached to the fireballs at the endpoints of the original firetube. Thus, the leading particle spectra are intimately related to the mass and rapidity distribution of these endpoint fireballs.

If we let  $w$  be the probability of firetube breaking per unit time,  $\sqrt{s}$  the initial center of mass energy,  $m$  the fireball mass and  $y$  the rapidity, then the end-point fireball spectra, in the limit  $\sqrt{s} \gg m_h$ , is given by

$$\left[ \frac{d^2 P}{dm dy} \right]_{EP} = \frac{mw}{k_{eff}^2} \exp \left[ -\frac{wm\sqrt{s}}{2k_{eff}^2} e^{\mp y} \right] \Theta(\mp y + y_{max}) \quad (9)$$

where the minus and plus signs of  $y$  refer to the fireball from the right and left, respectively,

$y_{\max} = \ln(\sqrt{s}/m)$ , and  $\Theta$  is the Heavyside function. The rapidity distribution of the end-point fireball can be obtained by integrating the above expression with respect to  $m$ . In practice, the finiteness of  $m_{th}$  (we took in this work  $m_{th} \simeq 1$  GeV) alters the spectrum especially for lower incident energies. In Fig.3, we show the rapidity distribution of the end-point fireballs for different incident energies. For higher energies, the distribution tends to that of Eq.(9).

In order to relate the fireball spectrum to that of the leading particle, we assume that the incident protons are detached from the fireball before the system enters in the thermal equilibrium if the mass of the fireball is not so large, say  $m \leq m_l$ . Such a process can be simulated by a mechanism similar to that of the firetube break up, except that the breaking occurs just at the position of the leading particle trajectory, leaving the minimum mass  $m_{th}$  for the remnant fireball. For  $m > m_l$ , we calculate the proton spectra with the prescription which is described later. However, the leading particle spectra is rather insensitive on the details of these decay modes, but essentially just depends only on the value of  $m_l$ , which was adjusted as  $\simeq 6$  GeV to reproduce the experimental data. In Fig.4, we show the calculated leading particle spectrum, together with the experimental values<sup>10-12</sup>. Adding the contribution from the diffractive process (dashed curve), the accordance between the calculated and the experimental spectra is fairly good. The diffractive contribution here is supposed to be 20 % of the total inelastic cross section. From this leading particle spectrum, we can calculate the inelasticity coefficient, defined as  $1 - \langle E \rangle / E_0$ , where  $\langle E \rangle$  is the average value of the final proton energy and  $E_0$  the incident energy. In Fig.5, we show the calculated inelasticity as a function of the incident energy. As can be seen from this figure, our model predicts the slow increase of the inelasticity coefficient with the incident energy. This behaviour is analogous to the dual string model<sup>13,14</sup> (See also the discussions in Refs. 15 and 16.)

## LONGITUDINAL EXPANSION OF FIREBALL

The hadron spectrum is calculated from the decay of the fireballs as the final stage of the model. Several alternative assumptions may be made to treat the decay processes. In Ref.<sup>3</sup> a statistical thermal model was considered, where the pion and kaon spectra in the center of mass of a fireball of mass  $m$  are given by

$$\frac{1}{\sigma_\pi} \frac{d^3 \sigma_\pi}{dp^3} = \frac{Z_\pi}{\pi} e^{-E_l \cosh(y)/T(m)}, \quad (10)$$

$$\frac{1}{\sigma_\kappa} \frac{d^3 \sigma_\kappa}{dp^3} = \frac{Z_\kappa}{\pi} e^{-E_l \cosh(y)/T(m)}. \quad (11)$$

where  $E = E_l \cosh(y)$  and  $p$  are the energy and momentum of the emitted particles and  $Z_{\pi,\kappa}$  is the normalization constant.

Here, the "temperature"  $T$  of a fireball should be considered as an effective one in the sense that it does not necessarily correspond to the real temperature at the time when the fireball dissociates into final free hadrons. It is merely a parameter which represents the exponential decay of the transverse spectra of final particles, and therefore many other non-thermal effects are possibly incorporated in this parameter, such as transverse expansion, final state interactions and non-equilibrium components. In fact, Hama and Navarra<sup>17</sup> argued that, while the actual dissociation temperature decreases as the mass of the fireball increases, the average transverse momenta of the final particles can increase due to the fluid dynamical effect of transverse expansion.

The effective temperature is parametrized as a function of the fireball mass by<sup>3</sup>,

$$T = \frac{m_\pi}{1 - 1.6\nu} \quad (12)$$

where

$$\nu = \frac{1.2(m^\nu - m_{th}^\nu)}{m^\nu + \sqrt{m^{2\nu} - 2.24m_{th}^\nu(m^\nu - m_{th}^\nu)}} \quad (13)$$

which simulates the behaviour of the transverse momentum  $\langle p_t \rangle$  as a power function of the fireball mass<sup>18</sup> with an exponent  $\nu$ . Here we take  $\nu$  as an adjustable parameter.

In order to treat the longitudinal expansion of the fireball, we suppose that the final hadron spectra is obtained as a convolution of the collective motion of the fireball elements and the thermal decay spectra of hadrons, like in the hydrodynamical model. In this case, the rapidity distribution of the fluid elements of the fireball can be well approximated by a Gaussian distribution<sup>19</sup>,

$$f(\bar{y}) \propto e^{-1/2\alpha\bar{y}^2} \quad (14)$$

which in turn can be approximated by

$$f(\bar{y}) = \frac{1}{2K_0(\alpha)} e^{-\alpha \cosh(\bar{y})} \quad (15)$$

where  $K_0$  is the Bessel function.  $\bar{y}$  stands for the rapidity of the fluid element and  $\alpha$  is a parameter related to the longitudinal energy of the fluid in the fireball.

The longitudinal expansion in the hydrodynamical model is relatively well studied, and we took the dependence of the parameter  $\alpha$  on the fireball mass as

$$\alpha = \frac{2}{\log(m/m_0)} \quad (16)$$

where  $m_0$  denotes the mass scale for which the longitudinal expansion starts.

In our model, fireballs which have the same mass  $m$  can be formed in different ways from firetubes of various thicknesses. A fireball formed from a thinner firetube has larger longitudinal kinetic energy than the one which are formed from a thicker firetube. Then, we expect that the former one should have the larger longitudinal expansion than the latter. In this mode, the parameter  $m_0$  should be related to a some quantity which measures how much the firetube, before the formation of the fireball, was elongated.

We then define the parameter  $m_0$  as the mass of the firetube whose initial longitudinal dimension  $L$  and transversal dimension  $R$  are related as

$$\alpha_0 = \frac{L}{R}$$

where  $\alpha_0$  is a parameter independent of the firetube. Since the longitudinal size  $L$  is given by

$$L \simeq \frac{m_0}{\epsilon_0 A(b, \sqrt{s})}$$

whereas the transversal size is given by

$$R \simeq \sqrt{\frac{A(b, \sqrt{s})}{\pi}}$$

we get

$$m_0 = \alpha_0 \epsilon_0 A^{3/2}(b, \sqrt{s}) \quad (17)$$

## HADRON SPECTRA

Once the temperature parameter  $T$  and longitudinal expansion coefficient  $\alpha$  are determined as a function of the fireball mass  $m$ , we calculate the pion spectra as

$$\begin{aligned} \frac{1}{\sigma_\pi} \frac{d^3 \sigma_\pi}{dp^3} &= \frac{Z_\pi}{\pi} \int_{-\infty}^{+\infty} d\bar{y} \frac{1}{2K_0(\alpha)} e^{-\alpha \cosh(\bar{y})} e^{-E_i \cosh(y-\bar{y})/T(m)} \\ &= \frac{Z_\pi}{K_0(\alpha)} K_0 \left( \sqrt{\alpha^2 + 2 \left( \frac{E_T}{T} \right) \alpha \cosh(y) + \left( \frac{E_T}{T} \right)^2} \right) \end{aligned} \quad (18)$$

where  $E_T$  is the transverse energy. For kaons and baryons, we have analogous expressions.

Note that for large  $\alpha$  we recover the isotropic decay inclusive spectrum, i.e.,

$$\left. \frac{Z_\pi}{K_0(\alpha)} K_0 \left( \sqrt{\alpha^2 + 2 \left( \frac{E_T}{T} \right) \alpha \cosh(y) + \left( \frac{E_T}{T} \right)^2} \right) \right]_{\infty} \longrightarrow \frac{Z_\pi}{\pi} e^{-E_i \cosh(y)/T(m)} \quad (19)$$

For a given mass  $m$ , the average multiplicity  $\bar{N}$  is determined by the normalization condition,

$$\begin{aligned}\bar{N}_{\pi,\kappa,B} &= \sum_{\pi,\kappa,B} \int d^3\vec{p} \frac{1}{\sigma} \frac{d^3\sigma}{dp^3} \\ &= 4Z_{\pi,\kappa,B} m_{\pi,\kappa,B} T K_1(m_{\pi,\kappa,B}/T)\end{aligned}\quad (20)$$

and the energy conservation,

$$\begin{aligned}m &= \sum_{\pi,\kappa,B} \int d^3\vec{p} \frac{E}{\sigma} \frac{d^3\sigma}{dp^3} \\ &= \frac{4K_1(\alpha)}{K_0(\alpha)} (Z_{\pi} m_{\pi}^2 T K_2(m_{\pi}/T) + Z_{\kappa} m_{\kappa}^2 T K_2(m_{\kappa}/T) + Z_B m_B^2 T K_2(m_B/T))\end{aligned}\quad (21)$$

where the subscripts,  $\pi, \kappa$  and  $B$  refer to pions, kaons and baryons, respectively. Neglecting baryon production in the decay process, we have  $N_B = 1$  for the fireball formed at the endpoints of the initial firetube, and  $N_B = 0$  for other fireballs in between. This simplification allows us to determine the normalization constant  $Z_B$  from Eq.(20). We are left with three equations for the four unknown variables,  $N_{\pi}, N_{\kappa}, Z_{\pi}, Z_{\kappa}$ . It is necessary to specify the relative abundance of kaons to pions. To determine the relative normalization of pions and kaons as a function of the fireball mass, we note that the  $K/\pi$  ratio should vanish for  $m \rightarrow 2m_{\kappa}$ , and should tend asymptotically to a some constant for  $m \rightarrow \infty$ . Thus, we introduce the following ansatz:

$$\frac{Z_{\kappa}}{Z_{\pi}} = \left(\frac{Z_{\kappa}}{Z_{\pi}}\right)_{\infty} \left(1 - \exp\left(-\frac{m - 2m_{\kappa}}{\xi}\right)\right), \quad (22)$$

where  $\left(\frac{Z_{\kappa}}{Z_{\pi}}\right)_{\infty}$  and  $\xi$  are taken as adjustable parameters.

With the help of the normalization conditions Eqs.(20-22), together with the condition  $N_B = 0$  or  $N_B = 1$ , the hadron spectra from a fireball of a given mass  $m$  can now be calculated completely ( Eq.(18) and analogous expressions for kaons and baryons).

The rapidity ( $y$ ) and the transverse momentum ( $p_t$ ) distributions of hadrons from a fireball are calculated by,

$$\frac{dN_{\pi,k}}{dy} = \int \frac{d^2 N_{\pi,k}}{dy dp_i^2} dp_i^2 \quad (23)$$

$$\frac{dN_{\pi,k}}{dp_i^2} = \int \frac{d^2 N_{\pi,k}}{dy dp_i^2} dy$$

With the above prescriptions for the decay of a fireball, the final-hadron spectra are then calculated by folding the fireball mass and rapidity distributions as,

$$\frac{dN_{\pi,k}}{dy} = \int_{m_{th}}^{m_{max}} dm \int_{-y_{max}}^{y_{max}} dy_{fb} \frac{dN}{dy_{\pi,k}} \frac{d^2 P}{dm dy_{fb}} \quad (24)$$

and

$$\frac{dN_{\pi,k}}{dp_i^2} = \int_{m_{th}}^{m_{max}} dm \int_{-y_{max}}^{y_{max}} dy_{fb} \frac{dN}{dp_{i^2,\pi,k}} \frac{d^2 P}{dm dy_{fb}} \quad (25)$$

The average total multiplicity of hadrons  $n_{\pi}$  and  $n_k$  are given by,

$$n_{\pi} = \int_{m_{th}}^{m_{max}} dm \langle n_{\pi}(m) \rangle \frac{dP}{dm_{fb}} \quad (26)$$

$$n_k = \int_{m_{th}}^{m_{max}} dm \langle n_k(m) \rangle \frac{dP}{dm_{fb}}$$

## CHARGED PARTICLES

Formulas in the preceding section refer to the hadron spectra without any distinction of charged states. However, the experimental data are usually concerned with the charged particles only. Therefore, it is necessary to convert our formulas to those for the charged particles. For this purpose, we simply assume that the fireballs which does not contain the incident proton carry always zero total charge, and that any charge state of mesons (pions and kaons) has the same probability. Thus, for these fireballs, we have

$$N_{\pi^{\pm}} = N_{\pi^0} = \frac{1}{3} N_{\pi}, \quad (27)$$

$$N_{K^{\pm}} = N_{K^0} = N_{\bar{K}^0} = \frac{1}{4} N_K$$

For fireballs which contain the incident protons, we assume that the proton transfers a half of its charge, in average, to mesons. The final charge configuration can be determined

by maximizing the number of ways of distributing this transferred positive charge between  $\pi^+$  and  $K^+$  under the constraints,

$$\begin{aligned} N_{\pi^+} + N_{\pi^-} + N_{\pi^0} &= N_{\pi} \\ N_{K^+} + N_{K^0} &= N_{K^-} + N_{K^0} = \frac{1}{2}N_K \\ N_{\pi^+} - N_{\pi^-} &= Q \end{aligned} \quad (28)$$

where  $Q$  is the transferred charge ( $= 1/2$ ). We found that the above condition leads to:

$$\begin{aligned} N_{\pi^0} &\simeq 1/3N_{\pi}, \\ Q^* &= Q\left(1 - \frac{1}{2}\frac{N_K}{N_{\pi}}\right), \\ N_{\pi^+} &= \frac{1}{2}(N_{\pi} + Q^* - N_{\pi^0}), \\ N_{\pi^-} &= \frac{1}{2}(N_{\pi} - Q^* - N_{\pi^0}), \\ N_{K^+} &= \frac{1}{4}(N_{\pi} + Q), \\ N_{K^0} &= \frac{1}{4}(N_{\pi} - Q), \end{aligned} \quad (29)$$

### III. RESULTS AND DISCUSSION

In the present model, the incident energy dependence of observable quantities enters only through the total inelastic cross section  $\sigma_{inel}(\sqrt{s})$  (geometrical scaling<sup>3</sup>). In the present analysis, we fitted the experimental values<sup>20-22</sup> of the cross section (see Fig.6) as a function of  $\sqrt{s}$  as

$$\sigma_{inel} = 26.55 + .577 \log \sqrt{s} + .46(\log \sqrt{s})^2 \quad (30)$$

After fixing the total cross section, we search the values of the parameters introduced in the previous section to fit the various observable quantities, such as total multiplicity, rapidity distribution, transverse momenta,  $K/\pi$  ratio, etc.

For the sake of bookkeeping, we list in the following, the adjustable parameters of the model and their physical meaning. These parameters are classified into two groups: one for the firetube dynamics and other the fireball decay into hadrons.

#### Parameters for Firetube

Parameter	Physical role	Expression
$\epsilon_0$	Volumetric energy density per parton	Eq.(1)
$\omega$	Probability density of firetube breaking	$\frac{d^2P}{dxdt}$
$m_{th}$	Threshold mass of fireballs	

It is worthwhile to mention that there exist a scaling relation<sup>3</sup> among the parameters  $\epsilon, \omega, m_{th}$  and the incident energy  $\sqrt{s}$ . In particular for higher energies, where the role of  $m_{th}$  becomes ineffective, the first two parameters are almost reduce into one parameter,  $\omega/\epsilon^2$ .

#### Parameters of Fireball Decay

Parameter	Physical role	Expression
$\alpha_0$	Mass scale parameter for longitudinal expansion	Eq.(17)
$\nu$	Mass dependence of the temperature $T(m)$	Eq.(13)
$(\frac{Z_A}{Z_A})_\infty, \xi$	Mass dependence of the $K - \pi$ ratio	Eq.(22)

Among these parameters, we simply fixed a priori the two of them:  $\omega = 0.01 \text{ fm}^{-2}$  and  $m_{th} = 1 \text{ GeV}$ . This is because some of the observable quantities are not sensible to these parameters.

Furthermore, for any change of the values of these parameters within an reasonable interval, we can always obtain the same good results as before by adjusting the others. Therefore, we use just the 5 parameters  $\epsilon_0, \alpha_0, \nu, (\frac{Z_\pi}{Z_\pi})_\infty$  and  $\xi$  to fit the  $K/\pi$  ratio, the (pseudo-) rapidity distributions and transverse momentum spectra. The first one,  $\epsilon_0$  is the only parameter related to the firetube fragmentation. The parameters  $\epsilon_0$  and  $\alpha_0$  are found to control essentially the overall multiplicity data, together with the temperature parameter  $\nu$ . This last parameter strongly affect the  $P_t$  distributions, as expected. To have a reasonable behaviour of the  $P_t$  spectra, we obtained

$$\nu \simeq \frac{1}{5}.$$

After fixing the temperature parameter to the above value, the other parameters,  $\epsilon_0, \alpha_0, (\frac{Z_\pi}{Z_\pi})_\infty$  and  $\xi$  are adjusted to reproduce the experimental data. In this manner, we obtained the following set of values:

$$\begin{aligned}\epsilon_0 &= 0.3 \\ \alpha_0 &= 0.02 \\ (\frac{Z_\pi}{Z_\pi})_\infty &= 0.15 \\ \xi &= 2.4\end{aligned}$$

In the following, we present the results calculated with the above values of the parameters.

### RAPIDITY (PSEUDO-RAPIDITY) DISTRIBUTION

The basic change introduced in this new version of the firetube model compared to the original one<sup>3</sup> is the longitudinal expansion of the fireballs. Since the transverse energies are much smaller than the longitudinal ones, we expect that this change will not influence much the rapidity spectra. In fact, as shown in Fig.7-(a,b), the calculated rapidity (or pseudo-rapidity) distributions stayed as good as those in Ref.3 reproducing well the experimental data<sup>21-25</sup> for all values of  $\sqrt{s}$  from 20 to 900 GeV.

For higher energies, only the pseudo-rapidity experimental distributions are available. For the sake of direct comparison, we converted our calculated rapidity spectra into those for pseudo-rapidity, using the approximate formula<sup>26</sup>,

$$\frac{dN}{d\eta} = \left[1 - \frac{m^2}{\langle E_t^2 \rangle \cosh y^2}\right]^{1/2} \frac{dN}{dy}$$

with

$$\eta = \frac{1}{2} \ln \frac{\cosh y \left[1 - \frac{m^2}{\langle E_t^2 \rangle \cosh y^2}\right]^{1/2} + \sinh y}{\cosh y \left[1 - \frac{m^2}{\langle E_t^2 \rangle \cosh y^2}\right]^{1/2} - \sinh y}$$

where  $\langle E_t^2 \rangle$  is the average transverse energy (see below).

An interesting point is that the pseudo-rapidity distribution for  $\sqrt{s} = 1800$  GeV ( Fig.7-c, curve 1 ) is found to be lower than the experimental data<sup>27</sup>. This indicates that the inelastic cross section at this energy might be greater than the value estimated by Eq.(30). At  $\sqrt{s} = 1800$  GeV, the extrapolation of our fitted cross section gives  $\sigma_{inel} = 56.7$  mb. If we take  $\sigma_{inel} = 67$  mb instead, we get a better fit of pseudo-rapidity distribution ( Fig.7-c, curve 2). It is worthwhile to investigate further on this point.

## TRANSVERSE MOMENTA

In Fig.8, we plotted the calculated  $\langle p_t \rangle$  as a function of the incident energy which shows an excellent agreement with the experimental data<sup>17,28-31</sup> for pions, although the agreement with the kaon data are not so good. In particular, a kind of discontinuity observed in the kaon data around  $\sqrt{s} \sim 200$  GeV is difficult to be reproduced in the present model. Note that the slow increase of  $\langle p_t \rangle$  for higher energies reflects the increase of the average fireball mass.

Figs.9-(a,b,c,d) show the comparison of the calculated spectra of pions and kaons with the corresponding experimental data. In all cases, the agreement is excellent.

## KAON TO PION RATIO

Fig.10 shows the comparison of the calculated  $K/\pi$  ratio with the experimental data<sup>29</sup> as a function the incident energy. In our model there are essentially two parameters,  $(\frac{Z}{Z^*})_{\infty}$ ,  $\xi$  to control this quantity. However, the ansatz Eq.(22) refers to the dependence of the ratio as a function of the fireball mas, not of the incident energy. Thus, the final value of the ratio depends on the mass distribution of the fireballs, which in turn reflects the dependence on the incident energy. The agreement of our curve to the experimental values is excellent.

## HADRON-PROTON COLLISIONS

It is interesting to apply our model to the other hadron-hadron collision process than the proton-(anti)proton case. Here, we calculate the rapidity distribution of negative pions for the pion-proton and kaon-proton collisions at  $p_{inc} = 250$  GeV/c. In the present calculation, the only change introduced for these cases was to use the value of the experimental inelastic cross sections<sup>20</sup> for each reaction, instead of the formula Eq.(30). All other values of parameters are kept equal to those of the previous results. Fig. 11 is the calculated rapidity distribution of negative charged particles, compared with the experimental data<sup>32</sup>. The agreement for proton-proton case is very good as expected. For the pion-proton reaction, the overall behaviour of the rapidity distribution is well reproduced by the simple substitution of the cross section value in our model, except for the small asymetry. For the kaon-proton reaction, our result becomes less satisfactory. These calculations suggest that the influence of the valence quarks, especially those of strange(heavy) quarks seems to violate the idea of the simple geometrical scaling at such lower energies. In the present model, the roles of the valence quarks are completely neglected.

#### IV. CONCLUDING REMARKS

In this paper, we developed some improvements of the firetube model. The main point is the introduction of the longitudinal expansion effect of the fireballs, which improved the behaviour of the transverse momenta of the final hadrons. The present version is found to reproduce almost all the global properties of the experimental inclusive observables of proton-(anti)proton reaction. Some semi-inclusive data, such as the two particle correlations in pseudo-rapidity space are also reproduced in this model. With a trivial extension of the model, it also reproduces reasonably well the rapidity distributions of pion-proton and kaon-proton reactions. These results are very satisfactory considering the simplicity of the model. We therefore expect that the extension of the present model to the more complex systems, as p-nucleus, or light nucleus-nucleus reactions will serve to describe the macroscopic aspects of the hadron productions, in particular, their peripheral collisions. These calculations are now under progress.

Several points deserve to be commented. We remind ourselves that the present model is concerned mainly with the macroscopic properties of the observable quantities, particularly with their dependence on the incident energy, without entering into the details of the incident hadron structure (no effects of valence quarks). All of these energy dependences come out as a consequence of the energy dependence of the total inelastic cross section. We found that the most of the data treated here fit with this vision, changing smoothly with the incident energy. However, some of them seem to be out of this scheme. The first one is the average transverse momenta of kaons. As is seen from Fig. 8, there seems to exist some abrupt change around  $\sqrt{s} \sim 200$  GeV. This discontinuous behaviour is also seen in the form of pseudo-rapidity distribution at this energy. Another one is the data at  $\sqrt{s} = 1800$  GeV. The smooth extrapolation of the inelastic cross section value to this energy fails to fit the observed pseudo-rapidity distribution. Some further investigation is necessary to understand these points.

**Acknowledgement** We deeply acknowledge the stimulating discussion with the colleagues of Rio-São Paulo Working Group on Hadron Interactions. In particular, our thanks go to Prof. Y.Hama for his valuable suggestions.

## FIGURE CAPTIONS

### Fig.1

- a - The mass distributions of fireballs generated by the firetube fragmentation for three different incident energies.
- b - The rapidity distributions of fireballs generated by the firetube fragmentation for three different incident energies.

**Fig.2** Short range correlations in pseudo-rapidity,  $C_s(\eta_1, \eta_2)$  for various incident energies, plotted as functions of  $\eta_2$ , with  $\eta_1 = 0$ . Data points are taken from Ref.8.

**Fig.3** The rapidity distribution of fireballs at the end-points of the firetube for three different incident energies.

**Fig.4** Leading particle spectra plotted as a function of the Feynmann  $x_F$  variable, defined as  $x_F = p_{\parallel}/p_0$ , where  $p_{\parallel}$  and  $p_0$  are, respectively, the final and initial proton longitudinal momenta. The dashed line is the result obtained by our model ( $\sqrt{s} = 20$  GeV). The dotted line shows the contribution of the diffractive process. The solid curve corresponds to the sum of these two contributions. Triangles and circles are data points<sup>10,11</sup>.

**Fig.5** Inelasticity coefficient as a function of the incident energy.

**Fig.6** Inelastic  $p - p(\bar{p})$  cross section as a function of the incident energy. The solid curve corresponds to the Eq.(30). The two crosses (1,2) are the values of the cross sections used in the calculations of the pseudo-rapidity distributions for  $\sqrt{s} = 1800$  GeV (see Fig.7-c). Experimental data are taken from Refs.20-22.

### Fig.7

- a - (Pseudo-) Rapidity distributions of charged particles for various energies. The two lower energy cases ( $\sqrt{s} = 20, 53$  GeV) refer the rapidity distributions, whereas the rest ( $\sqrt{s} = 200, 540, 900$  GeV) refer to the pseudo-rapidity distributions. Data points are taken from Refs. 21-24.
- b - Rapidity distributions of negatively charged particles for energies  $\sqrt{s} = 30$  GeV and 44 GeV. Data points are taken from Ref. 25.
- c - Pseudo-rapidity distribution of charged particles for  $\sqrt{s} = 1800$  GeV. The curve 1 is the result obtained with the cross section extrapolated by the Eq.(30) (cross 1 in Fig.6). The curve 2 corresponds to the value of the cross section indicated by the cross 2 in Fig.6. Data points are taken from Ref.27.

**Fig.8** Average transverse momentum of produced particles as a function of the incident energy. The solid curve (calculated) and the squares (experimental) refer to pion data. The dashed curve (calculated) and the triangles (experimental) refer to kaon data.

**Fig.9**

- a - Pion spectra at  $y = 0$  plotted as function of  $P_t$ .
- b - Kaon spectra at  $y = 0$  plotted as function of  $P_t$ .
- c - Pion spectra, averaged in the rapidity interval  $-2.5 < y < 2.5$ , plotted as function of  $P_t$ .
- d - Kaon spectra, integrated in the rapidity interval  $-2.5 < y < 2.5$ , plotted as function of  $P_t$ .

**Fig.10**  $K/\pi$  ratio plotted as a function of the incident energy. The solid curve is the result of the calculation. The squares are the experimental data of Ref.29.

**Fig. 11** Rapidity distributions of negative charged particles for  $p+p, \pi^+ + p$  and  $K^+ + p$  reactions at  $p_{lab} = 250$  GeV/c. The histograms represent the respective experimental data<sup>32</sup>.

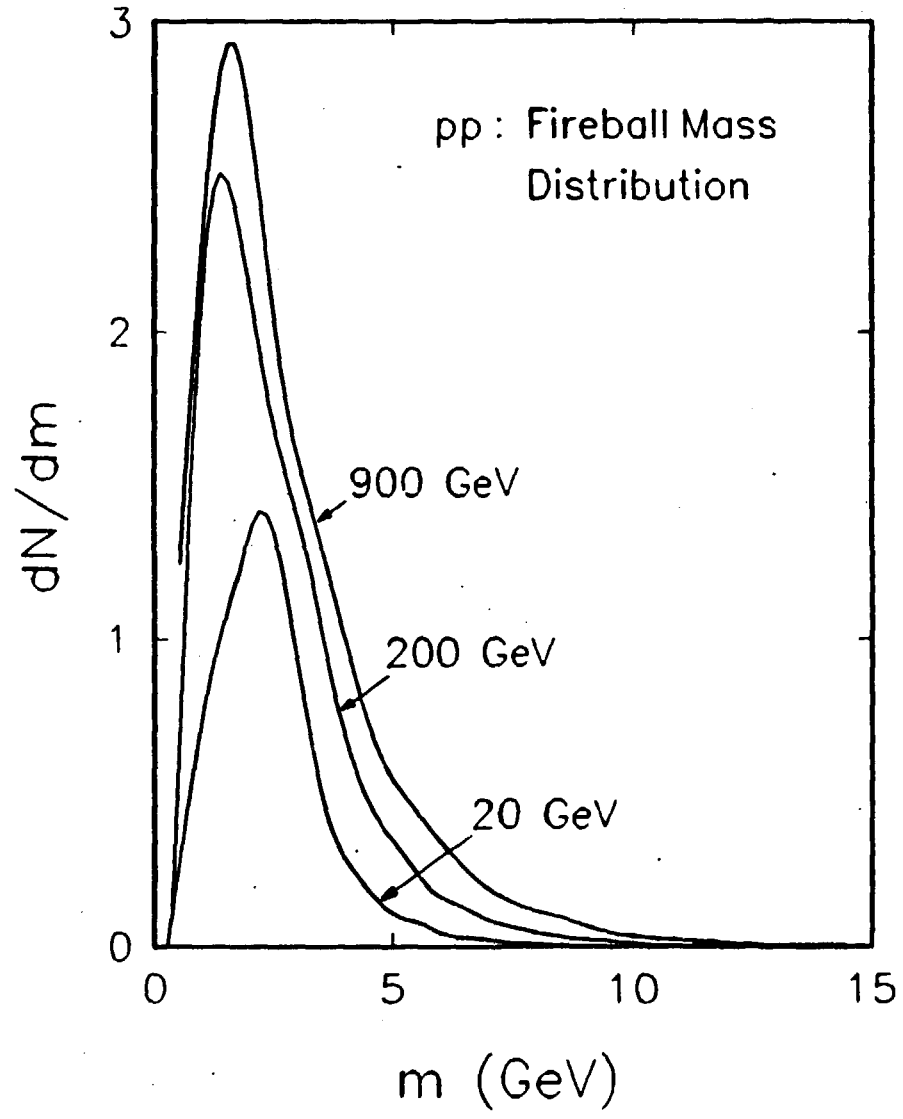


FIG. 1-a

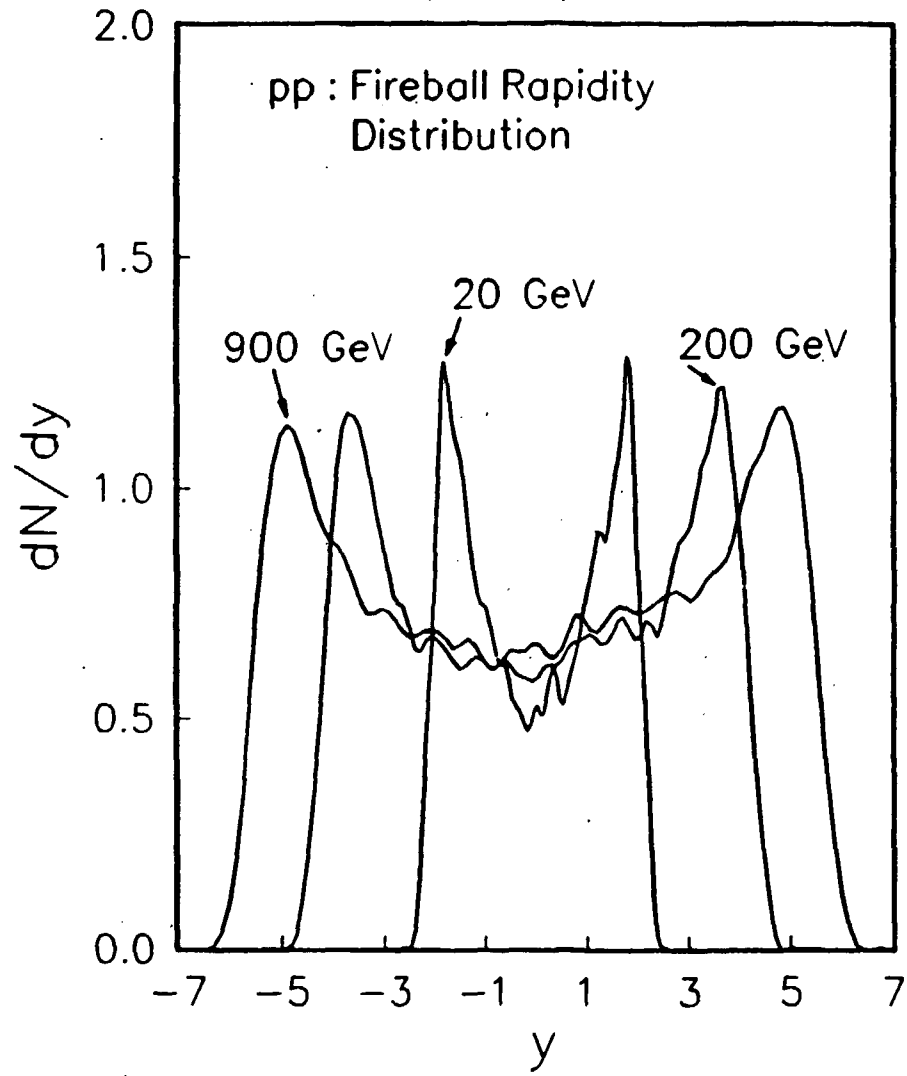


FIG. 1-b

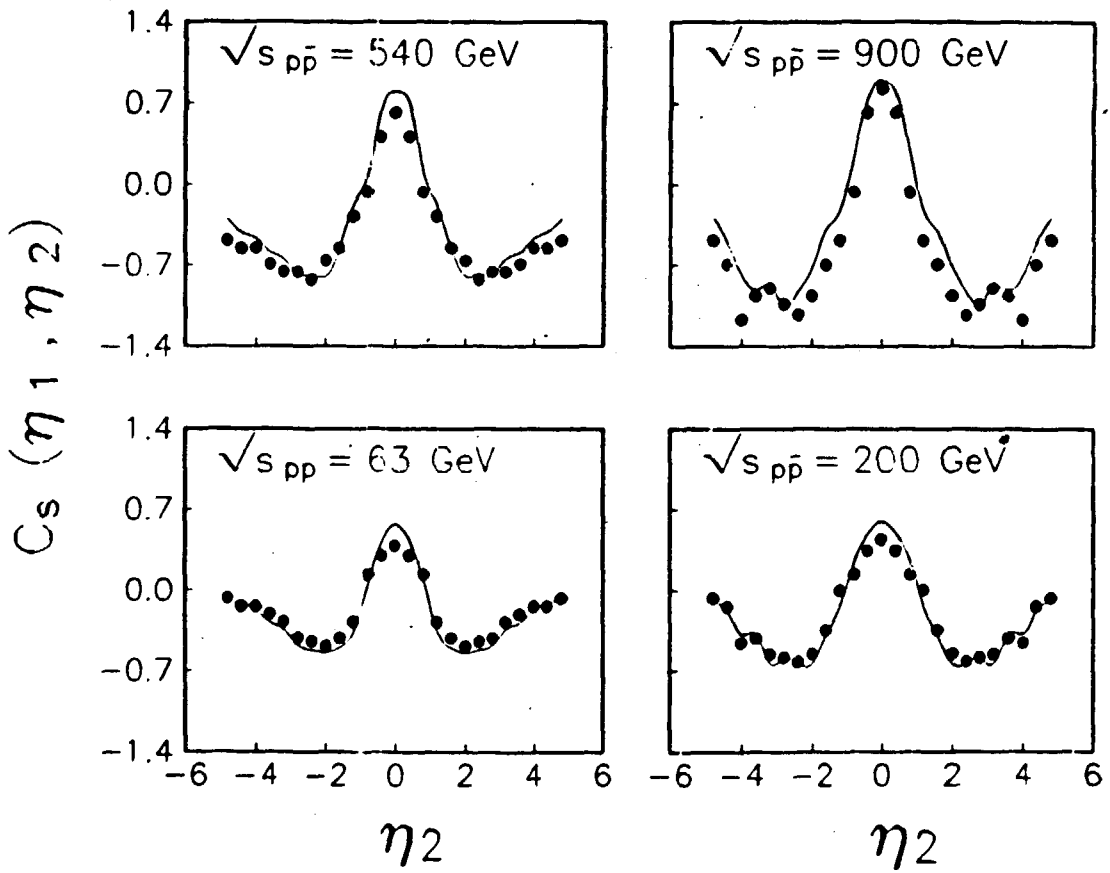


FIG. 2

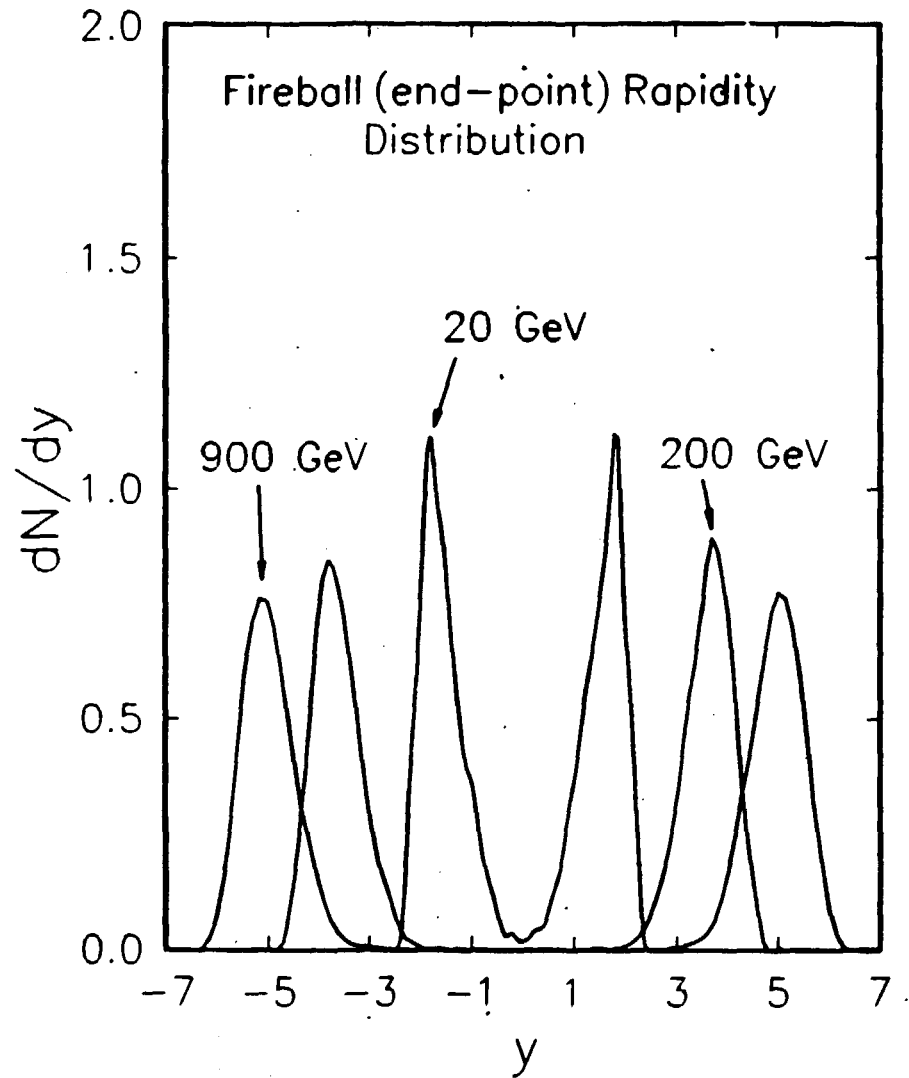


FIG. 3

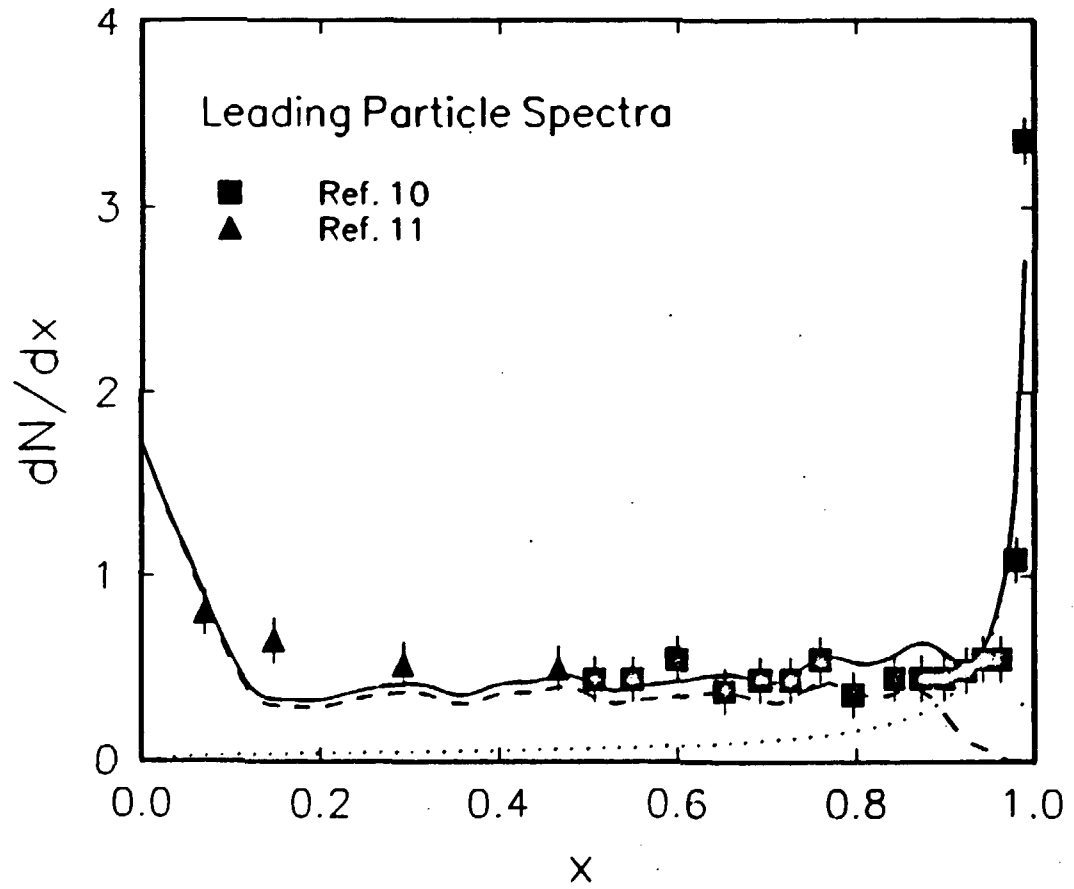


FIG. 4

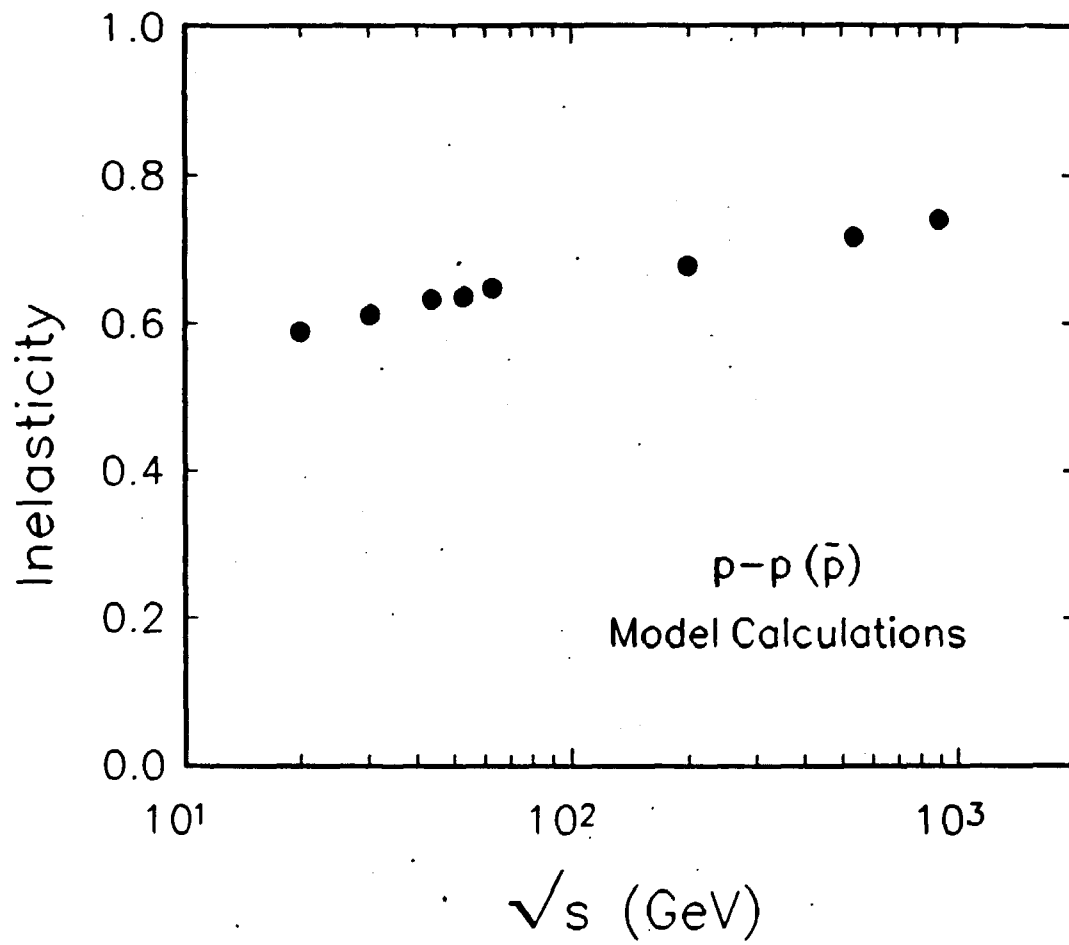


FIG. 5

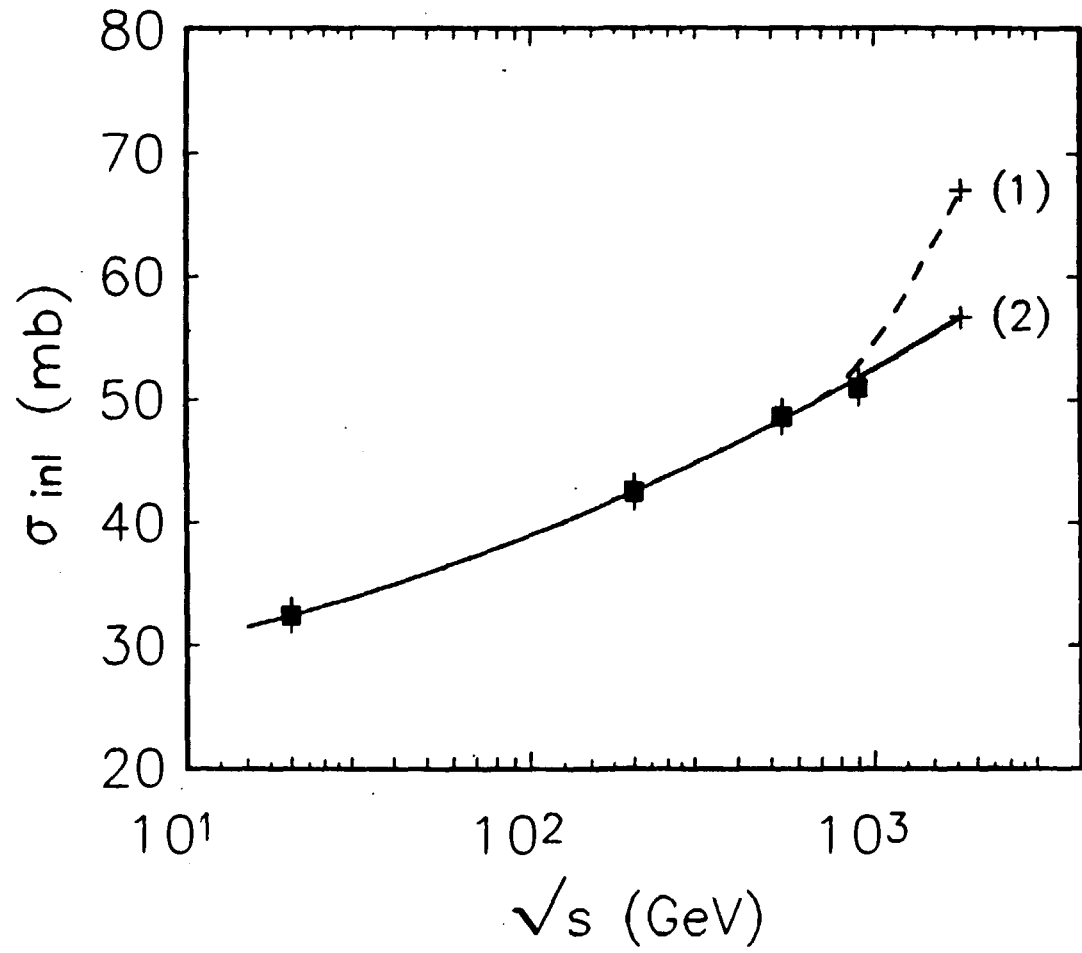


FIG. 6

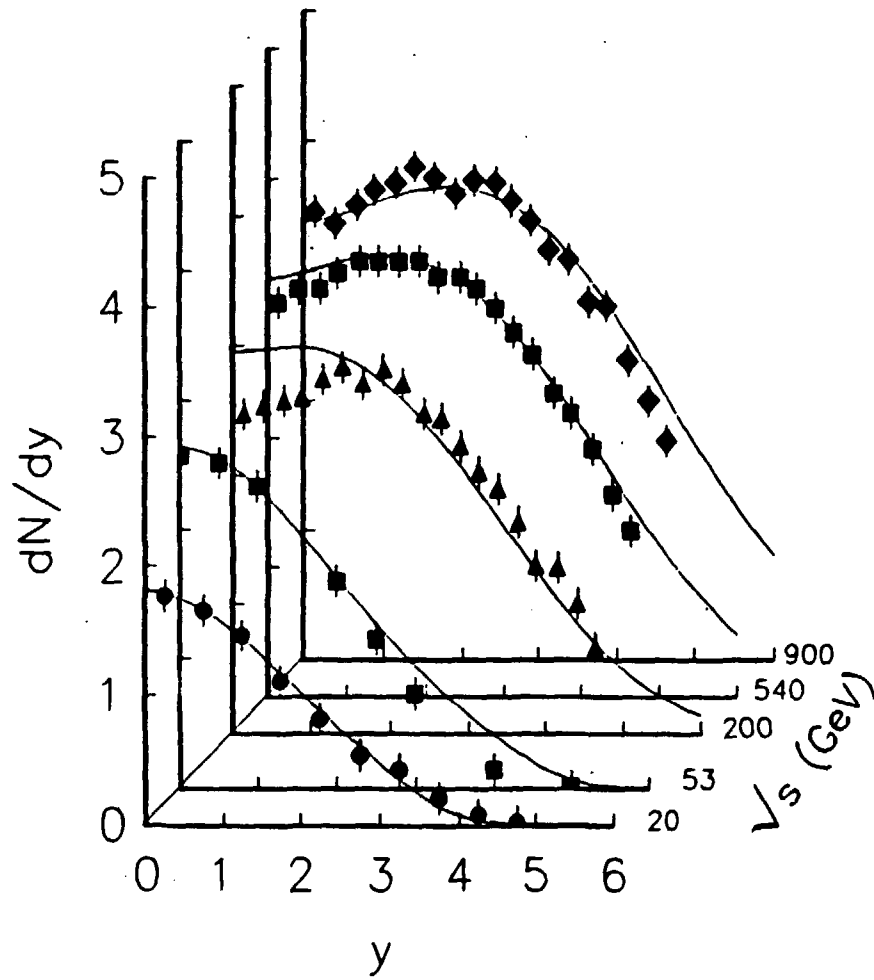


FIG. 7-a

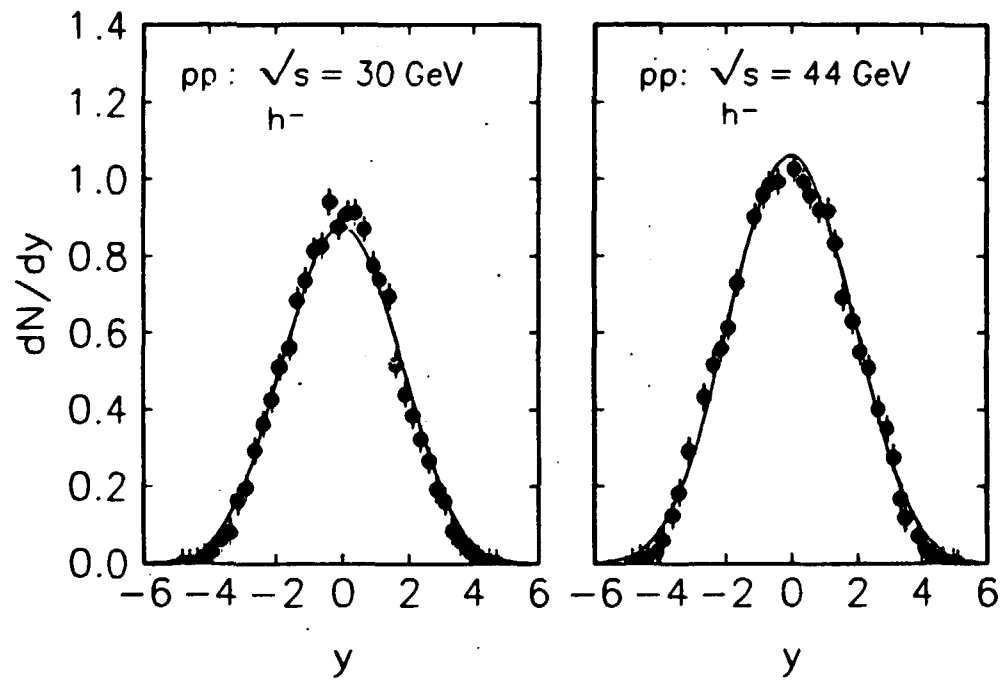


FIG. 7-b

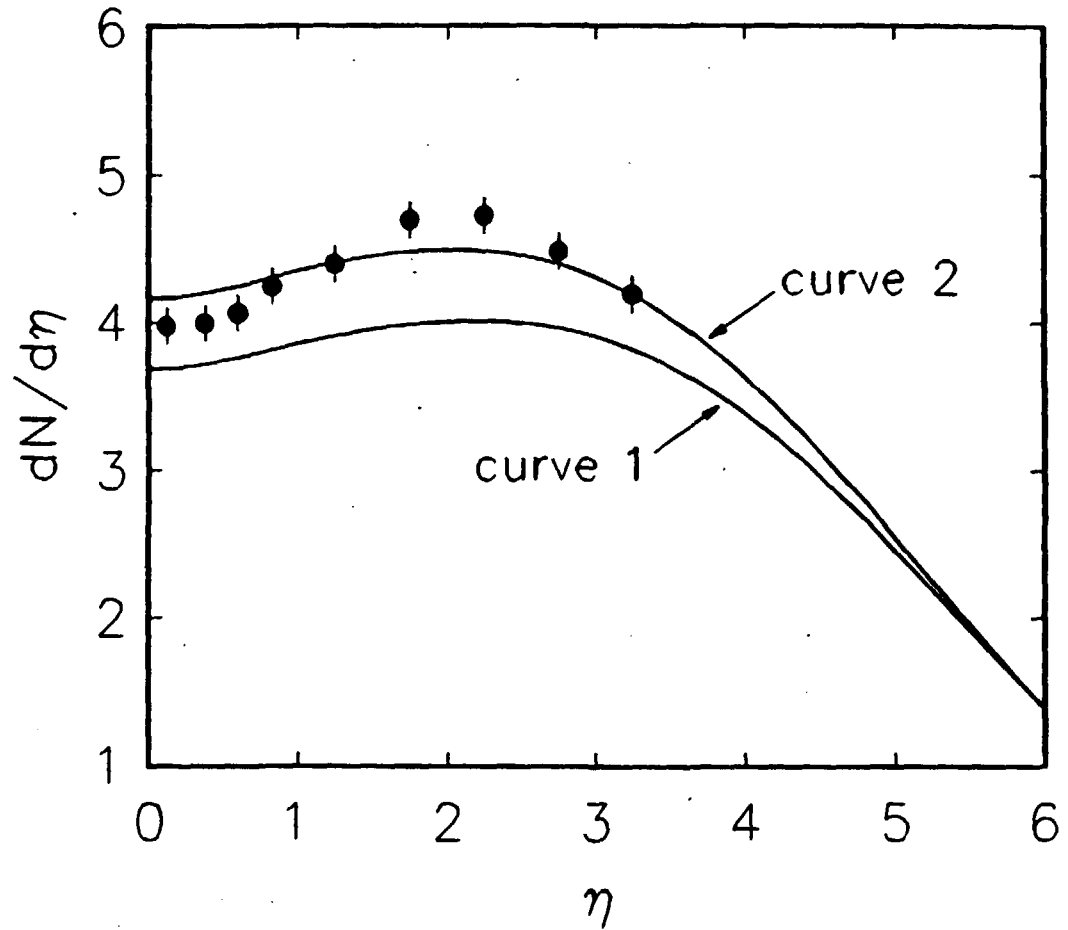


FIG. 7-c

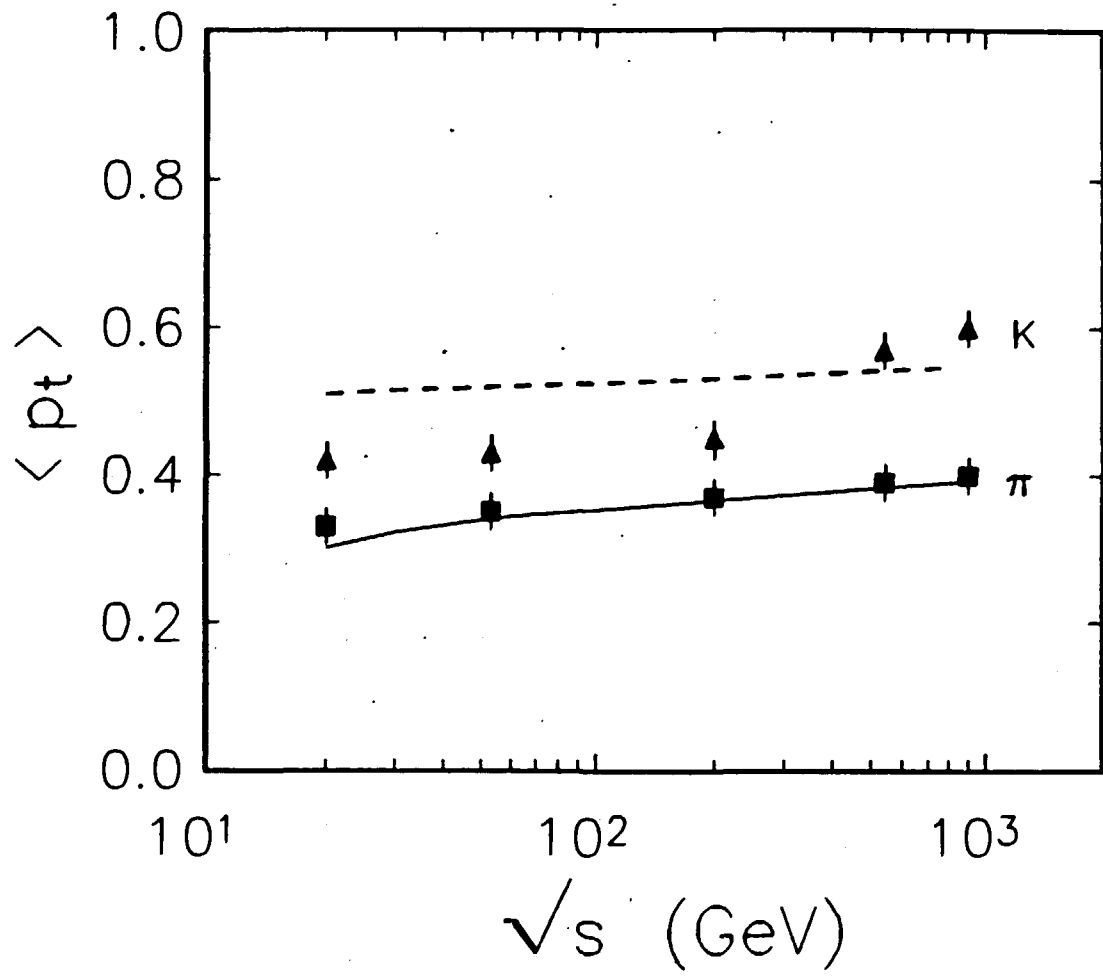


FIG. 8

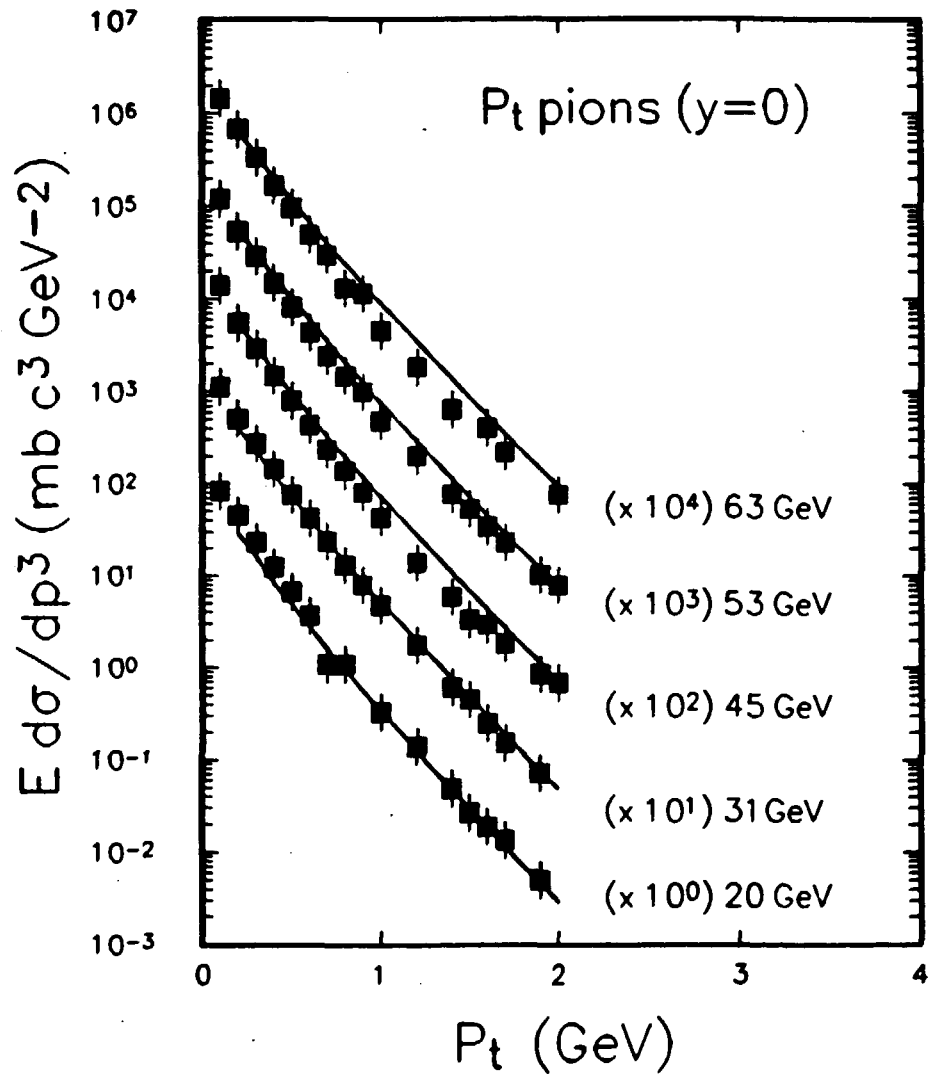


FIG. 9-a

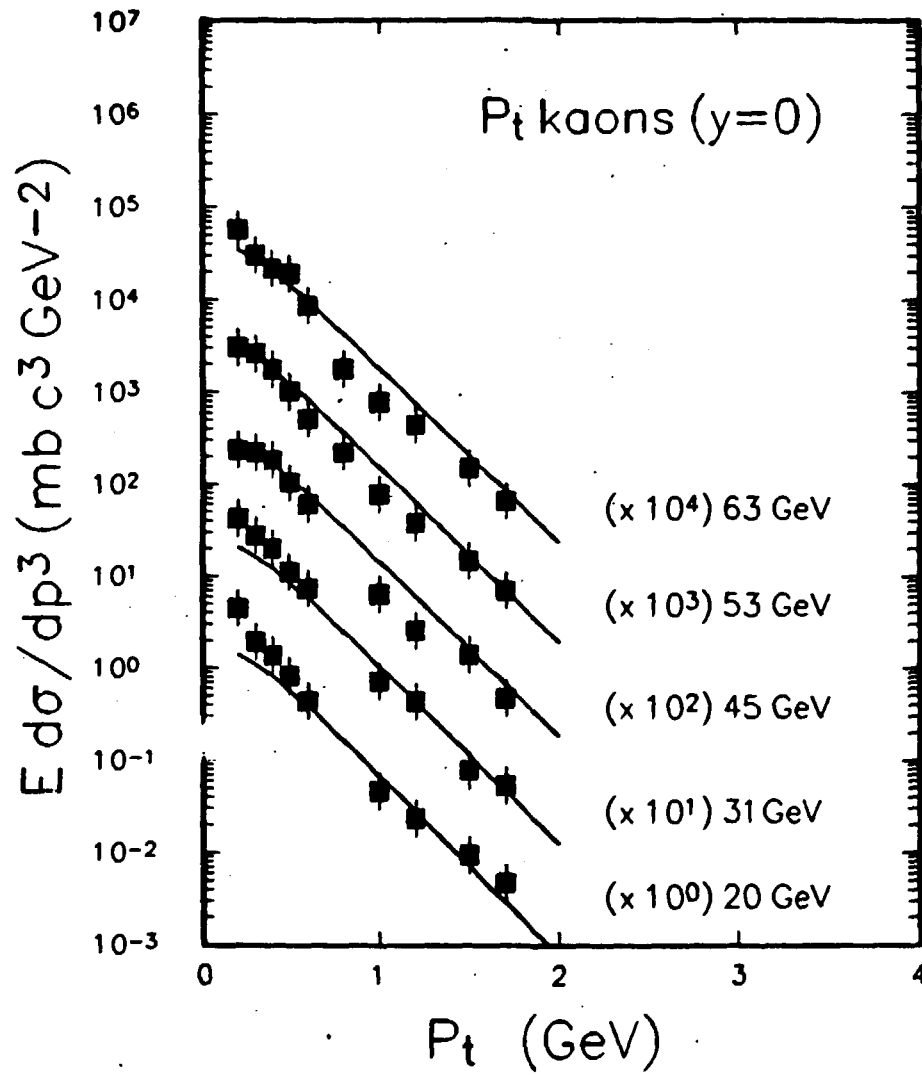


FIG. 9-b

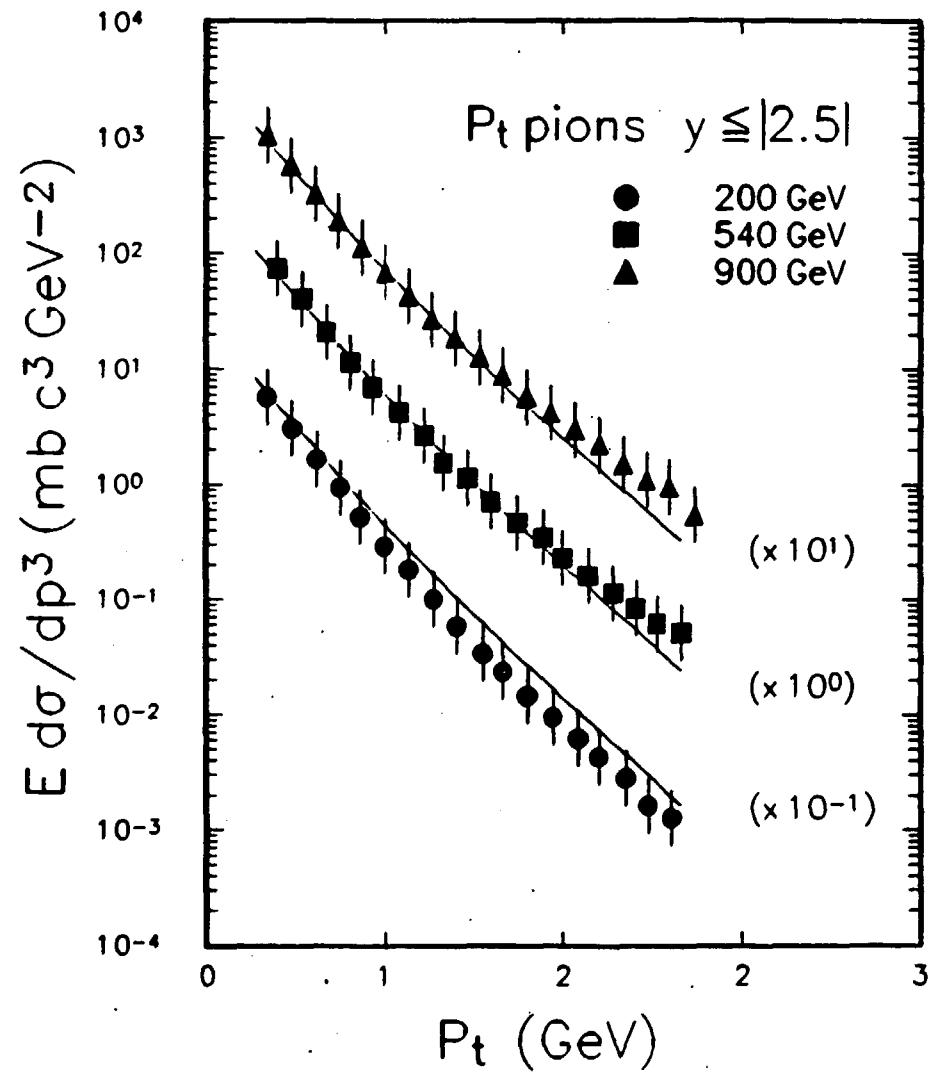


FIG. 9-c

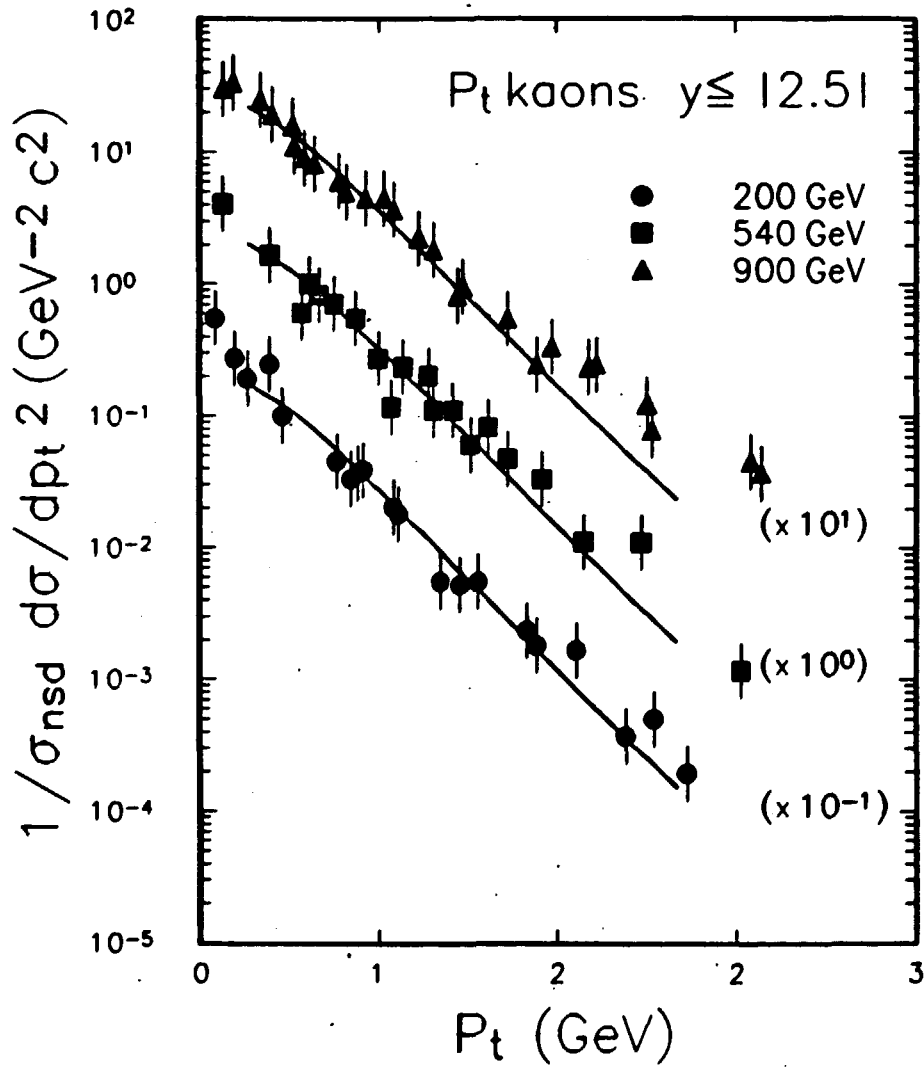


FIG. 9-d

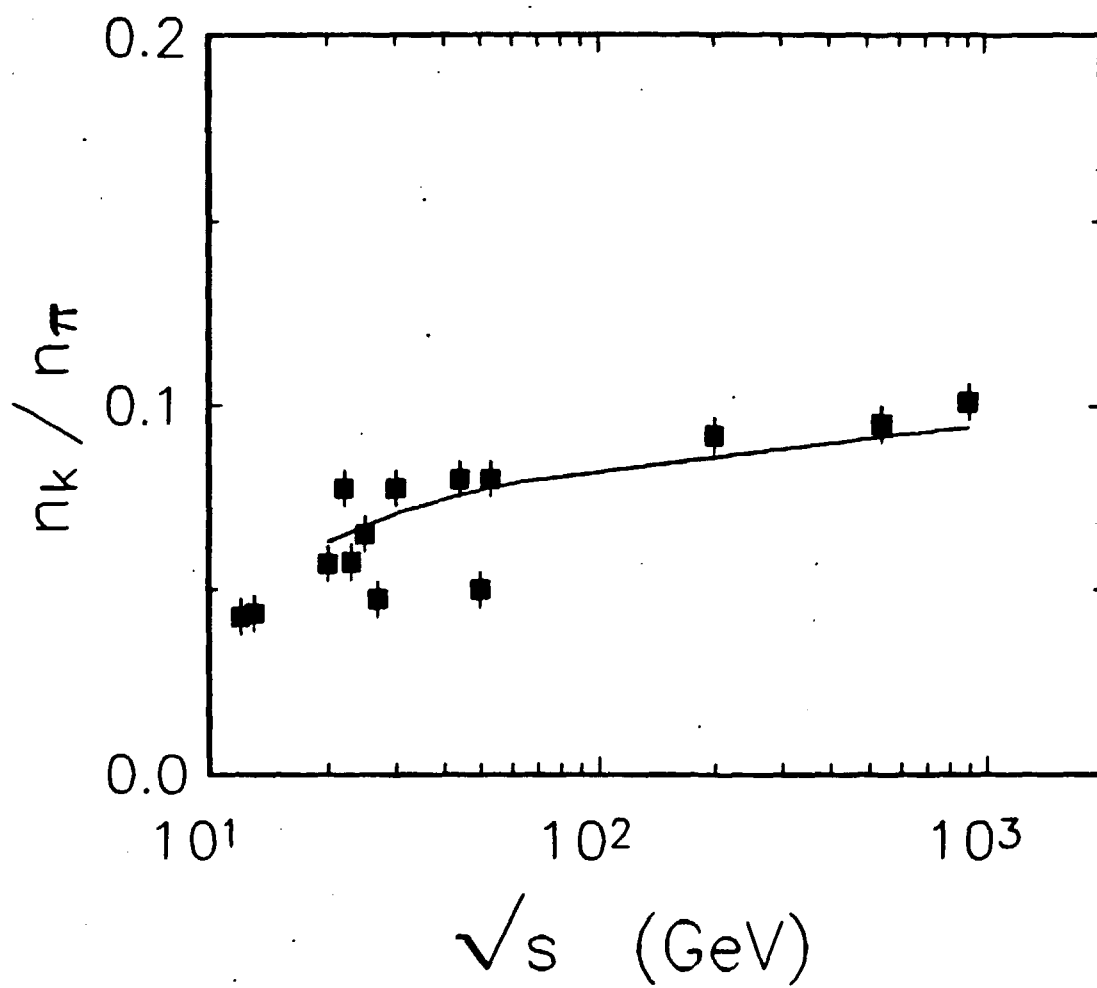


FIG. 10

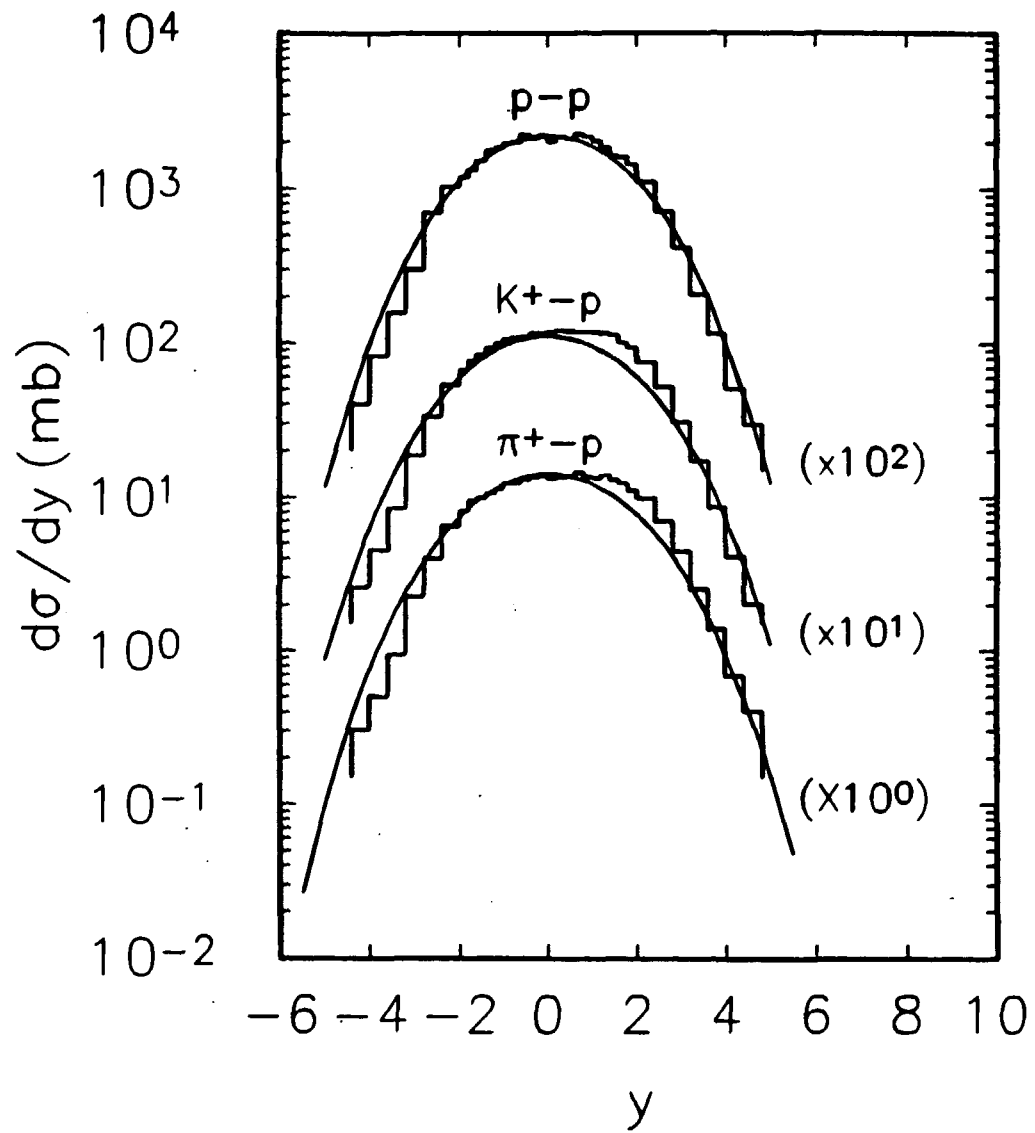


FIG. 11

### References

1. N. Prado, R. A. M. S. Nazareth, and T. Kodama, *Rev. Bras. Fis.* **16** (1986) 452 .
2. N. Prado, Ph.D. Thesis, Institute of Physics, UFRJ (1989).
3. R. A. M. S. Nazareth, N. Prado and T. Kodama, *Phys. Rev.* **D40** (1989) 1628.
4. X. Artru and G. Mennesier, *Nucl. Phys.* **B70**, 93 (1971); B. Andersson, G. Gustafson, G. Ingelman, T. Sjöstrand and X. Artru, *Phys. Rev.* **97** (1983) 31.
5. A two-step mechanism was also suggested for  $e - \bar{e}$  jet phenomena by T. D. Gottschalk, *Nucl. Phys.* **B239** (1984) 349.
6. F.E. Low, *Phys. Rev.* **D12** (1975) 163.
7. E.L. Berger, *Nucl. Phys.* **B85** (1975) 61.
8. G.J. Alner *et al* (UA5 Collaboration), *Phys. Report* **154**, 247 (1987); R. Singer *et al*, *Phys. Rev.* **D16** (1977) 1261; S.R. Amendolia *et al*, *Nuovo Cim.* **31 A** (1976) 17; R.E. Ansorge *et al* (UA5 Collaboration), *Z. Phys.* **C37** (1988) 191
9. D. A. Portes Jr., Thesis, *Centro Brasileiro de Pesquisas Físicas*, Rio de Janeiro, 1991
10. P. Cappilupi *et al.*, *Nucl. Phys.* **B70** (1974) 1.
11. J.W. Chapman *et al.*, *Phys. Rev. Lett.* **32** (1974) 257.
12. M. Basile *et al*, *Lett. Nuovo Cim.* **38** (1983) 359.
13. A. Kaidalov and K.A. Ter Matrirusian, *Phys. Lett.* **117B** (1982) 247.
14. S. Barshay and Y. Chiba, *Phys. Lett.* **167B** (1986) 449.
15. J. N. Capedevielle, *J. Phys. G*, **15** (1989) 909.
16. A. Ohsawa and K. Sawayanagi, ICRR-Report-257-91-26 ( Univ. Tokyo )
17. Y.Hama and F.S. Navarra, *Z.Phys. C* (1991), in press.
18. G. A. Kilekhin, *Zh. E.T.F.* **35** (1958) 1185.
19. Y. Hama, *Phys. Rev.* **D19** (1979) 2623.

20. NA22 Collaboration, M. Adamus et al., Z. Phys. C32 (1986) 475.
21. UA5 Collaboration, G. J. Alner et al., Phys. Rep.154 (1987) 247.
22. UA5 Collaboration, G. J. Alner et al., Z. Phys.C33 (1986) 1.
23. C. De Marzo et al., Phys. Rev. D26 (1982) 1019 .
24. A. Breakstone et al., Phys. Lett. 132B (1983) 458 .
25. W. Bell et al., Z. Phys. C27 (1985) 191.
26. C-Y. Wong, Phys. Rev. D32 (1985) 94 .
27. F. Abe et al., Phys. Rev. (Rapid Comm.) D41 (1990) 2330.
28. G.J. Alner et al., Nucl. Phys. B258 (1985) 505.
29. B. Alper et al., Nucl. Phys. B100 (1975) 237.
30. R.E. Ansorge et al., Phys. Lett. B199 (1987) 311.
31. G. Arnison et al., Phys. Lett. B118 (1982) 167.
32. EHS-NA22 Collaboration, M. Adamus et al., Z. Phys. C39 (1988) 311.